PREPRINT

blank

Time-domain modelling of interconnects with highly oscillatory sources

Abstract

Purpose
The paper explores a new approach for time-domain modelling of interconnects with highly oscillatory modulated sources.
Design/methodology/approach
The paper employs an asymptotic method in conjunction with the Green's function of the Telegrapher's Equations. The Green's function is expressed as a series of rational functions in the Laplace domain and these are converted to pole-residue form thereby enabling time-domain implementation.
Findings
The results indicate that the method is accurate for modelling interconnects when widely-varying frequencies are present in the sources.
Originality/value
The technique is important in circuit design for assessing signal integrity and in electromagnetic compatibility testing.

Keywords: Transmission-lines, Time-domain models, Electrical circuits, Modulated signals.

1 Introduction

Modelling of interconnects is important in circuit design as signal integrity may be seriously degraded owing to interconnect effects such as signal delay, distortion and attenuation. Numerous approaches have been proposed for modelling interconnects —see (Achar 2011) for an overview. With ever rising frequencies, interconnects can no longer be modelled as short circuits or with lumped segment models. In addition, the ability to model *nonuniform* interconnects is becoming more and more important as package interconnects on printed circuit boards can have varying geometries (Antonini 2012). In addition, they have many applications in the microwave field (Yamamoto, Azakami & Itakura 1967). However, while transmission-line behaviour is best described in the frequency domain and while some frequency-domain modelling approaches such as (Moreno, Gómez, Naredo & Guardado 2005) and (Nagaoka & Ametani 1988) have been proposed, in practice, time-domain models are generally employed in circuit simulators for ease of interconnection with nonlinear elements. In addition, some frequency-domain models become complex when handling non-uniform transmission lines (Tang & Mao 2008). Some time-domain approaches for nonuniform interconnects are the two-step perturbation technique in (Chernobryvko, De

Zutter & Vande Ginste 2014), the finite-difference time-domain technique in (Afrooz & Abdipour 2012), the time-step integration method in (Tang & Mao 2008), the Lax-Wendroff difference method in (Dou & Dou 2011), the implicit Wendroff method in (Brančík & Ŝevčík 2011) and (Brančík 2011), the finite element method of (Jurić-Grgić, Lucić & Bernadić 2015) and the spectral methods of (Antonini 2012). In this paper, an approach is proposed for the case when the signals on the interconnects have widely-varying frequency content and as such present major challenges for numerical simulation. Meeting the Courant-Friedrich Lewy condition for the Finite Difference Time-Domain method would require very small time steps. Making simplifying assumptions regarding the nature of the input between time steps would lead to inaccuracies for such signals unless the time step was very small. Issues regarding the choice of time step also arise in employing a basic finite element method. The goal is to adapt models for the efficient simulation of modulated signals or signals with widely-varying frequency content on interconnects. This is important in electromagnetic compatibility testing (Afrooz & Abdipour 2012) and communication system analysis.

The proposed technique employs the concepts presented in (Altinbaçsak, Condon, Deaño & Iserles 2013) in conjunction with that in (Antonini 2012) and in related works by its author. The paper is concerned with modulated signals on interconnects and thus widely-varying frequency content is present.

2 Oscillatory sources on uniform transmission lines

2.1 The general framework

The Telegrapher's Equations for a multi-conductor transmission line are

$$\begin{aligned} \partial_x \boldsymbol{v}(x,t) &= -\boldsymbol{R}\boldsymbol{i}(x,t) - \boldsymbol{L}\partial_t \boldsymbol{i}(x,t) \\ \partial_x \boldsymbol{i}(x,t) &= -\boldsymbol{C}\partial_t \boldsymbol{v}(x,t) + \boldsymbol{i_s}(x,t) \end{aligned}$$

Eliminating $\boldsymbol{i}(x,t)$ and rearranging yields

$$\partial_x^2 \boldsymbol{v}(x,t) = \boldsymbol{LC}\partial_t^2 \boldsymbol{v}(x,t) + \boldsymbol{RC}\partial_t \boldsymbol{v}(x,t) - \boldsymbol{R}\boldsymbol{i_s}(x,t) - \boldsymbol{L}\partial_t \boldsymbol{i_s}(x,t) \quad x \in [0,l], \quad t \geq 0. \tag{2.1}$$

where $\boldsymbol{R}$, $\boldsymbol{L}$ and $\boldsymbol{C}$ are the per unit length resistance, inductance and capacitance matrices of the transmission line. The matrices are of size $N \times N$, when there are $N+1$ conductors in the multiconductor transmission line, one of which is the reference. $\boldsymbol{v}(x,t)$ and $\boldsymbol{i}(x,t)$ are the voltage and current vectors at position x at time t, respectively. The length of the line is l and $\boldsymbol{i}_s(x,t)$ are the per unit length current sources. We assume that currents are only injected into the system at $x=0$ and $x=l$.

Let the current source consist of a modulated signal:

$$\boldsymbol{i_{sx}}(x,t) = \sum_{n=-\infty}^{\infty} \boldsymbol{i_{sxn}}(x,t) e^{\mathrm{i}n\omega t} \quad t \geq 0,$$

$$
\begin{aligned}
\boldsymbol{i_{sx}}(x,t) &= \boldsymbol{i_{s0}}(t)\delta(x) + \boldsymbol{i_{sl}}(t)\delta(x-l), \\
\boldsymbol{i_{s0}}(t) &= \sum_{n=-\infty}^{\infty} \boldsymbol{i_{s0n}}(t)e^{\mathrm{i}n\omega t} \qquad t \geq 0, \\
\boldsymbol{i_{sl}}(t) &= \sum_{n=-\infty}^{\infty} \boldsymbol{i_{sln}}(t)e^{\mathrm{i}n\omega t} \qquad t \geq 0.
\end{aligned}
$$

We assume for simplicity that the functions, $\boldsymbol{i_{s0n}}(t)$ and $\boldsymbol{i_{sln}}(t)$ are all analytic. Moreover, we assume that the functions $\boldsymbol{i_{s0n}}(t)$ and $\boldsymbol{i_{sln}}(t)$ decay sufficiently rapidly for $|n| \gg 1$, rendering the infinite sum convergent. ω is the frequency of the high-frequency carrier signal.

We seek a solution of (2.1) of the form

$$
\boldsymbol{v}(x,t) = \sum_{n=-\infty}^{\infty} \boldsymbol{v_n}(x,t)e^{\mathrm{i}n\omega t} \quad t \geq 0, \quad x \in [0,l]. \tag{2.2}
$$

Substituting (2.2) into (2.1) and separating frequencies results in

$$
\begin{aligned}
&\boldsymbol{LC}\left(\partial_t^2 \boldsymbol{v_n}(x,t) + 2\mathrm{i}n\omega\partial_t \boldsymbol{v_n}(x,t) - n^2\omega^2 \boldsymbol{v_n}(x,t)\right) + \boldsymbol{RC}\left(\partial_t \boldsymbol{v_n}(x,t) + \mathrm{i}n\omega \boldsymbol{v_n}(x,t)\right) \\
&\quad = \partial_x^2 \boldsymbol{v_n}(x,t) + \boldsymbol{R}\boldsymbol{i_{sxn}}(x,t) + \boldsymbol{L}\mathrm{i}n\omega \boldsymbol{i_{sxn}}(x,t) + \boldsymbol{L}\partial_t \boldsymbol{i_{sxn}}(x,t) \quad x \in [0,l], \quad t \geq 0.
\end{aligned} \tag{2.3}
$$

2.2 The computation of $\boldsymbol{v_n}(x,t)$

To compute $\boldsymbol{v_n}(x,t)$, we convert equation (2.3) to the Laplace domain and rearrange.

$$
\begin{aligned}
&\partial_x^2 \boldsymbol{V_n}(x,s) - s^2 \boldsymbol{LC}\boldsymbol{V_n}(x,s) - s(\boldsymbol{RC} + 2\mathrm{i}n\omega\boldsymbol{LC})\boldsymbol{V_n}(x,s) \\
&-(\boldsymbol{RC}\mathrm{i}n\omega - \boldsymbol{LC}n^2\omega^2)\boldsymbol{V_n}(x,s) = -\boldsymbol{R}\boldsymbol{I_{sxn}}(x,s) - \boldsymbol{L}\mathrm{i}n\omega\boldsymbol{I_{sxn}}(x,s) - s\boldsymbol{L}\boldsymbol{I_{sxn}}(x,s)
\end{aligned}
$$

or

$$
\partial_x^2 \boldsymbol{V_n}(x,s) = \boldsymbol{\gamma^2}(s)\boldsymbol{V_n}(x,s) + \boldsymbol{b_n}(x,s) \tag{2.4}
$$

where

$$
\boldsymbol{\gamma^2}(s) = s^2\boldsymbol{LC} + s(\boldsymbol{RC} + 2\mathrm{i}n\omega\boldsymbol{LC}) + (\boldsymbol{RC}\mathrm{i}n\omega - n^2\omega^2\boldsymbol{LC})
$$

and

$$
\boldsymbol{b_n}(x,s) = -\boldsymbol{R}\boldsymbol{I_{sxn}}(x,s) - \boldsymbol{L}\mathrm{i}n\omega\boldsymbol{I_{sxn}}(x,s) - s\boldsymbol{L}\boldsymbol{I_{sxn}}(x,s).
$$

The solution to (2.4) is

$$\boldsymbol{V_n}(x,s) = \int_0^l \boldsymbol{G_n}(x,x',s)\boldsymbol{b_n}(x',s)dx'$$

where $\boldsymbol{G_n}(x,x',s)$ is the Green's function for (2.4).
$\boldsymbol{G_n}(x,x',s)$ can be expanded as

$$\boldsymbol{G_n}(x,x',s) = \sum_{m=0}^{\infty} \boldsymbol{a_m}(x',s)\phi_m(x)$$

where $\boldsymbol{a_m}$ is the matrix of amplitude coefficients.

As the currents at $x = 0$ and $x = l$ are treated as sources, the voltages satisfy homogeneous Neumann-type boundary conditions. Consequently, the set of eigenfunctions $\phi_m(x)$ satisfy the following differential equation subject to Neumann boundary conditions

$$\frac{d^2}{dx^2}\phi_m(x) + \lambda_m\phi_m(x) = 0$$

Hence, the eigenvalues and eigenfunctions are

$$\lambda_m = \left(\frac{m\pi}{l}\right)^2, \qquad \phi_m = A_m \cos\frac{m\pi x}{l}$$

where

$$A_m = \sqrt{\frac{1}{l}}, \quad m = 0,$$
$$A_m = \sqrt{\frac{2}{l}}, \quad m > 0.$$

The Green's function for (2.4) is a solution of the equation

$$\frac{d^2}{dx^2}\boldsymbol{G_n}(x,x',s) - \boldsymbol{\gamma^2}(s)\boldsymbol{G_n}(x,x',s) = \delta(x,x')\boldsymbol{I_N} \tag{2.5}$$

where $\delta(x,x')$ is the 1-D Dirac delta function and where $\boldsymbol{I_N}$ is the identity matrix of dimension N. We substitute the expansion for $\boldsymbol{G_n}(x,x',s)$ into (2.5), multiply by $\phi_k(x)$ and integrate from 0 to l. Since

$$\int_0^l \phi_m(x)\phi_k(x)dx = \delta_{m,k},$$

it follows that

$$\left[-\lambda_m \boldsymbol{I_N} - \boldsymbol{\gamma^2}(s)\right] \boldsymbol{a_m}(x',s) = \left[-(\frac{m\pi}{l})^2 \boldsymbol{I_N} - \boldsymbol{\gamma^2}(s)\right] \boldsymbol{a_m}(x',s) = \phi_m(x')\boldsymbol{I_N},$$

hence

$$\boldsymbol{a_m}(x',s) = -\left[\boldsymbol{\gamma^2}(s) + \left(\frac{m\pi}{l}\right)^2 \boldsymbol{I_N}\right]^{-1} \phi_m(x')\boldsymbol{I_N}.$$

This results in

$$\boldsymbol{G}(x,x',s) = -\sum_{m=0}^{\infty} \left[\boldsymbol{\gamma^2}(s) + \left(\frac{m\pi}{l}\right)^2 \boldsymbol{I_N}\right]^{-1} A_m^2 \left[\cos\left(\frac{m\pi x}{l}\right)\cos\left(\frac{m\pi x'}{l}\right)\right].$$

Hence, the voltages at $x = 0$ and $x = l$ are

$$\begin{aligned}
\boldsymbol{V_n}(0,s) &= \int_0^l \boldsymbol{G}(0,x',s)\left(-\boldsymbol{R} - s\boldsymbol{L} - \boldsymbol{L}\mathrm{i}n\omega\right)\boldsymbol{I_{sxn}}(x',s)dx' \\
&= \boldsymbol{G}(0,0,s)(-\boldsymbol{R} - s\boldsymbol{L} - \boldsymbol{L}\mathrm{i}n\omega)\boldsymbol{I_{s0n}}(s) + \boldsymbol{G}(0,l,s)(-\boldsymbol{R} - s\boldsymbol{L} - \boldsymbol{L}\mathrm{i}n\omega)\boldsymbol{I_{sln}}(s) \\
&= \sum_{m=0}^{\infty} \left[\gamma^2(s) + (\frac{m\pi}{l})^2\boldsymbol{I_N}\right]^{-1} A_m^2 \times \\
&((\boldsymbol{R} + s\boldsymbol{L} + \boldsymbol{L}\mathrm{i}n\omega)\boldsymbol{I_{s0n}}(s) + \cos(m\pi)(\boldsymbol{R} + s\boldsymbol{L} + \boldsymbol{L}\mathrm{i}n\omega)\boldsymbol{I_{sln}}(s))\,,
\end{aligned}$$

$$\begin{aligned}
\boldsymbol{V_n}(l,s) &= \int_0^l \boldsymbol{G}(l,x',s)(-\boldsymbol{R} - s\boldsymbol{L} - \boldsymbol{L}\mathrm{i}n\omega)\boldsymbol{I_{sxn}}(x',s)dx' \\
&= \boldsymbol{G}(l,0,s)(-\boldsymbol{R} - s\boldsymbol{L} - \boldsymbol{L}\mathrm{i}n\omega)\boldsymbol{I_{s0n}}(s) + \boldsymbol{G}(l,l,s)(-\boldsymbol{R} - s\boldsymbol{L} - \boldsymbol{L}\mathrm{i}n\omega)\boldsymbol{I_{sln}}(s) \\
&= \sum_{m=0}^{\infty} \left[\boldsymbol{\gamma^2}(s) + (\frac{m\pi}{l})^2\boldsymbol{I_N}\right]^{-1} A_m^2 \quad \times \\
&((\boldsymbol{R} + s\boldsymbol{L} + \boldsymbol{L}\mathrm{i}n\omega)\cos(m\pi)\boldsymbol{I_{s0n}}(s) + (\boldsymbol{R} + s\boldsymbol{L} + \boldsymbol{L}\mathrm{i}n\omega)\boldsymbol{I_{sln}}(s))\,,
\end{aligned}$$

respectively. Thus, the matrix representation for the *nth* terms in the expansion in (2.2) in the Laplace domain is

$$\begin{bmatrix} \boldsymbol{V_n}(0,s) \\ \boldsymbol{V_n}(l,s) \end{bmatrix} = \begin{bmatrix} \boldsymbol{Z_{n11}}(s) & \boldsymbol{Z_{n12}}(s) \\ \boldsymbol{Z_{n21}}(s) & \boldsymbol{Z_{n22}}(s) \end{bmatrix} \begin{bmatrix} \boldsymbol{I_{s0n}}(s) \\ \boldsymbol{I_{sln}}(s) \end{bmatrix}$$

where

$$\boldsymbol{Z_{n11}}(s) = \sum_{m=0}^{\infty} \left[\boldsymbol{\gamma^2}(s) + \left(\frac{m\pi}{l}\right)^2 \boldsymbol{I_N}\right]^{-1} A_m^2 \left[\boldsymbol{R} + \boldsymbol{L}\mathrm{i}n\omega + s\boldsymbol{L}\right],$$

$$\boldsymbol{Z_{n12}}(s) = \sum_{m=0}^{\infty} (-1)^m \left[\boldsymbol{\gamma^2}(s) + \left(\frac{m\pi}{l}\right)^2 \boldsymbol{I_N}\right]^{-1} A_m^2 \left[\boldsymbol{R} + \boldsymbol{L}\mathrm{i}n\omega + s\boldsymbol{L}\right],$$

$$\boldsymbol{Z_{n21}}(s) = \sum_{m=0}^{\infty} (-1)^m \left[\boldsymbol{\gamma^2}(s) + \left(\frac{m\pi}{l}\right)^2 \boldsymbol{I_N}\right]^{-1} A_m^2 \left[\boldsymbol{R} + \boldsymbol{L}\mathrm{i}n\omega + s\boldsymbol{L}\right],$$

$$\boldsymbol{Z_{n22}}(s) = \sum_{m=0}^{\infty} \left[\boldsymbol{\gamma^2}(s) + \left(\frac{m\pi}{l}\right)^2 \boldsymbol{I_N}\right]^{-1} A_m^2 \left[\boldsymbol{R} + \boldsymbol{L}\mathrm{i}n\omega + s\boldsymbol{L}\right].$$

Each $\boldsymbol{Z_{nij}}(s)$ is expressed as a sum of rational functions in s, hence the time-domain response can be determined by converting the representation into a state-space representation. The number of terms in the summations is set in practice to N_{mod} and this number is determined by the accuracy requirements.

Once each term $\boldsymbol{v_n}(x,t)$ is determined, the overall response can be determined as

$$\boldsymbol{v}(x,t) = \sum_{n=-\infty}^{\infty} \boldsymbol{v_n}(x,t)e^{\mathrm{i}n\omega t}.$$

2.3 Example 1

Consider a transmission line of length 0.3m. The per-unit parameters are $L = 50nH/m$, $C = 100pF/m$ and $R = 2\Omega/m$. Let the input current source be a modulated sine wave

$$I_s(t) = \sin(\omega_1 t)\sin(\omega t) \qquad t \geq 0$$

where $\omega_1 = 200\pi$ rad/s is the frequency of the slowly-varying signal that modulates the high-frequency signal. $\omega = 2\pi \times 10^6$ rad/s is the frequency of the high-frequency carrier signal.
Fig. 2.1 shows the absolute value of the terms in $Z_{n11}(s)$ for the given parameters at $f = 100Hz$ as a function of m and confirms that the terms decay rapidly with m. Fig. 2.2 depicts the voltage at the sending-end of the open-circuit transmission line. The dotted line is the result from the proposed method with N_{mod} set equal to 50. The solid line is the result obtained from an accurate numerical inverse Laplace transform analysis (Wilcox 1978). The Z or Y-parameters of the transmission line are formed in the Laplace domain and the required voltage in the Laplace domain is determined based on the boundary conditions. This is then converted to the time domain using the numerical inverse Laplace transform. However, what is important to note is that to simulate the system for a longer interval of time requires a very large number of discretization steps for the numerical inverse Laplace transform. The time-step must be small enough to capture the high frequency. This results in a very large

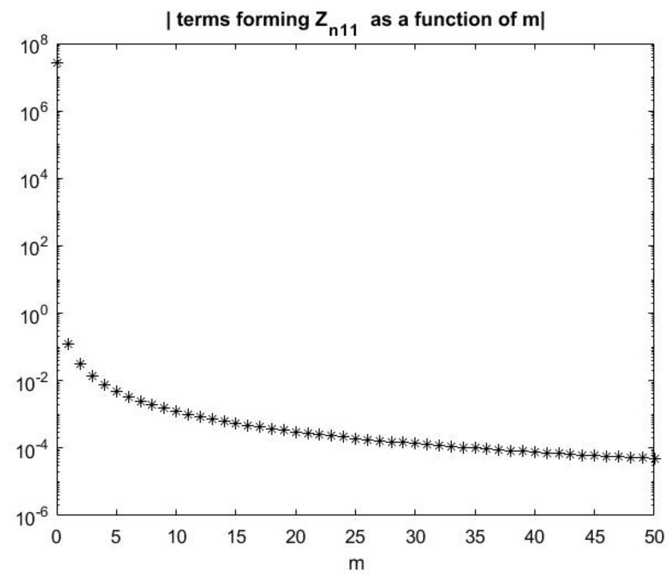

Figure 2.1: The decay of the terms forming $Z_{n11}(s)$ as a function of m.

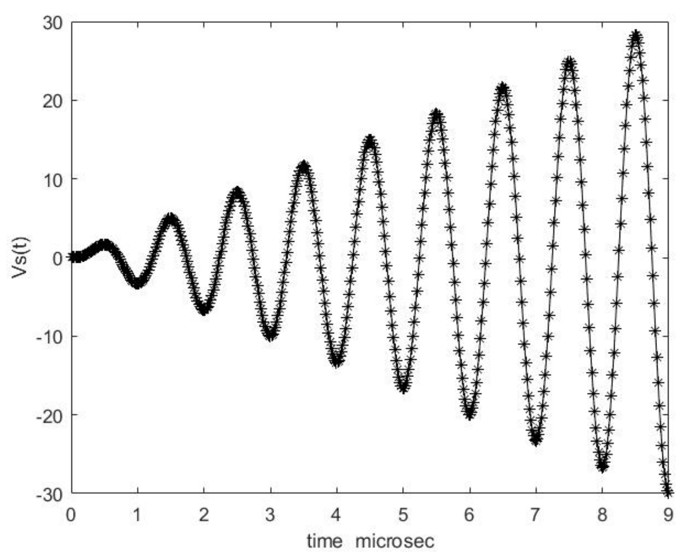

Figure 2.2: The voltage at the sending-end of the open-circuit transmission line.

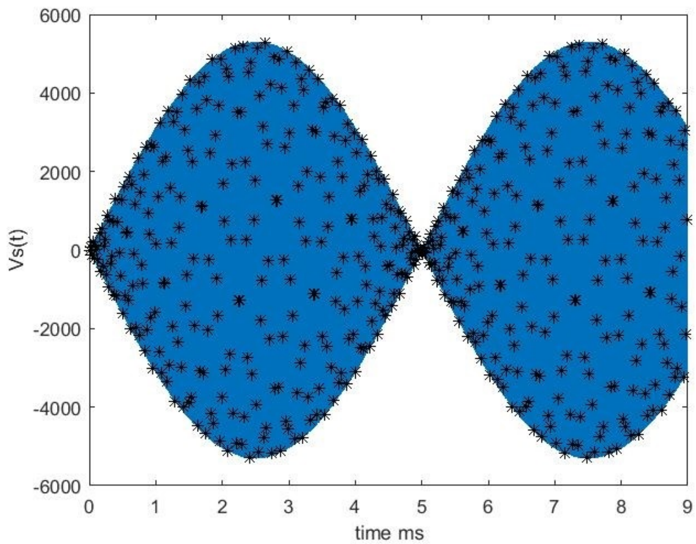

Figure 2.3: The voltage at the sending-end of the open-circuit transmission line on a longer time interval.

number of time steps to simulate even one cycle of the low-frequency information signal. However, with the proposed method, this is avoided as the high-frequency carrier is separated out. Hence, the greater the efficiency of the proposed method. Fig. 2.3 shows the same voltage waveform on a longer time interval.

2.4 Example 2

The second example is that when a non-linearity is present. A non-linear resistor is present at the sending end of the transmission line. In addition, there is a resistor of 1Ω in parallel with it. The equation governing the nonlinear resistor is

$$i(t) = 0.2v^2(t)$$

Fig. 2.4 depicts the voltage at the sending-end of the open-circuit transmission line. The dotted line is the result from the proposed method with N_{mod} set equal to 1. The solid line is the result obtained from an implementation of the Wendroff method similar to that in (Brančík & Ŝevčík 2011). The source current for this example is

$$I_s(t) = \sin(\omega_1 t)\sin(\omega t) \qquad t \geq 0$$

where $\omega_1 = 200\pi$ rad/s and $\omega = 2\pi \times 10^6$ rad/s. The length of the line is 0.003m. The per unit length parameters are $L = 50nH/m$, $C = 100pF/m$ and $R = 200\Omega/m$.

It should be noted that a nonlinearity results in coupling of the various v_n and i_n modes. This results in coupled nonlinear differential equations. However, the high-frequency signals are still separated from the low-frequency components so the gains in efficiency remain.

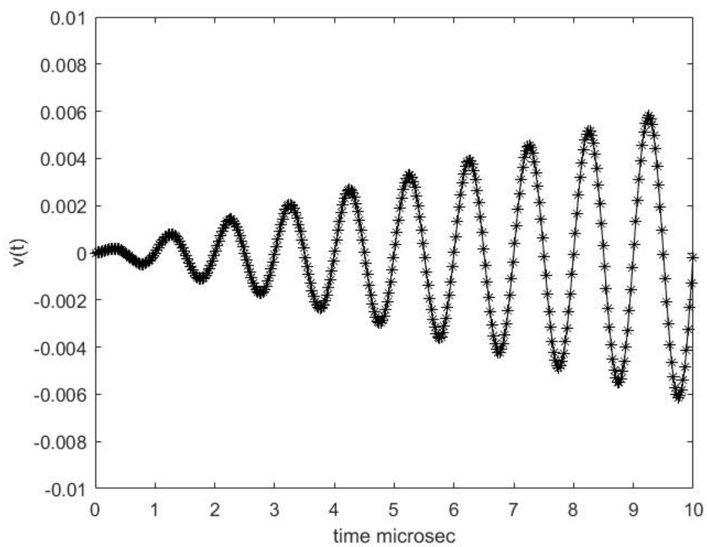

Figure 2.4: The voltage at the sending-end of the open-circuit transmission line when a nonlinearity is present.

3 Non-uniform transmission lines

In general, apart from a few special cases such as a linear variable non-uniform transmission line (Lu 1997), there are no exact solutions for non-uniform transmission lines. Several methods have been proposed: (Tang & Mao 2007), (Manfredi, De Zutter & Vande Ginste 2016), (Khalaj-Amirhosseini 2006), (Jurić-Grgić et al. 2015), (Afrooz & Abdipour 2012), (Antonini 2012) and many more. In this work, we adapt the approach presented for uniform lines in the above section for non-uniform transmission lines. The starting point is again the Telegrapher's Equations. In the Laplace domain, they are written as

$$\begin{aligned}\frac{d}{dx}\boldsymbol{V}(x,s) &= -\boldsymbol{R}(x)\boldsymbol{I}(x,s) - s\boldsymbol{L}(x)\boldsymbol{I}(x,s)\\ \frac{d}{dx}\boldsymbol{I}(x,s) &= -s\boldsymbol{C}(x)\boldsymbol{V}(x,s) + \boldsymbol{I_s}(x,s)\end{aligned}$$

Eliminating $\boldsymbol{I}(x,s)$ and rearranging yields

$$
\begin{aligned}
&\frac{d^2}{dx^2}\boldsymbol{V}(x,s) - (s^2\boldsymbol{L}(x)\boldsymbol{C}(x) + s\boldsymbol{R}(x)\boldsymbol{C}(x))\boldsymbol{V}(x,s) \\
&-(\boldsymbol{R}(x)+s\boldsymbol{L}(x))^{-1}\frac{d}{dx}(\boldsymbol{R}(x)+s\boldsymbol{L}(x))\frac{d}{dx}\boldsymbol{V}(x,s) = -(\boldsymbol{R}(x)+s\boldsymbol{L}(x))\boldsymbol{I_s}(x,s)
\end{aligned}
\tag{3.1}
$$

where $\boldsymbol{R}(x)$, $\boldsymbol{L}(x)$ and $\boldsymbol{C}(x)$ are the per unit length parameter matrices.

Now as for the uniform case, the proposed form of the solution is

$$\boldsymbol{v}(x,t) = \sum_n \boldsymbol{v_n}(x,t)e^{\mathrm{i}n\omega t} \quad t \geq 0, \quad x \in [0,l]. \tag{3.2}$$

Hence, the equation for each nth mode is

$$
\begin{aligned}
\frac{d^2}{dx^2}\boldsymbol{V_n}(x,s) - \boldsymbol{L}(x)\boldsymbol{C}(x)\left[s^2 + 2\mathrm{i}n\omega s - n^2\omega^2\right]\boldsymbol{V_n}(x,s) \\
- \left[s\boldsymbol{C}(x)\boldsymbol{R}(x) + \mathrm{i}n\omega\boldsymbol{C}(x)\boldsymbol{R}(x)\right]\boldsymbol{V_n}(x,s) \\
-(\boldsymbol{R}(x)+s\boldsymbol{L}(x)+\boldsymbol{L}(x)\mathrm{i}n\omega)^{-1}\frac{d}{dx}(\boldsymbol{R}(x)+s\boldsymbol{L}(x)+\boldsymbol{L}(x)\mathrm{i}n\omega)\frac{d}{dx}\boldsymbol{V_n}(x,s) \\
= -(\boldsymbol{R}(x)+s\boldsymbol{L}(x)+\boldsymbol{L}(x)\mathrm{i}n\omega)\boldsymbol{I_{sn}}(x,s)
\end{aligned}
\tag{3.3}
$$

The solution to 3.3 is

$$\boldsymbol{V_n}(x,s) = -\int_0^l \boldsymbol{G_n}(x,x',s)(\boldsymbol{R}(x')+s\boldsymbol{L}(x')+\boldsymbol{L}(x')\mathrm{i}n\omega)\boldsymbol{I_{sn}}(x',s)dx'$$

where $\boldsymbol{G_n}(x,x',s)$ is the Green's function.

Determination of the eigenvalues and eigenfunctions for 3.3, even if possible, is challenging (Antonini 2012). However, if the degree of non-uniformity is relatively small as is required so that only TEM mode propagation exists, the non-uniform line may be considered as a perturbation of the uniform line. Therefore, as in the method of (Antonini 2012), the eigenfunctions and eigenvalues that were used for the uniform line shall also be employed for the non-uniform interconnect.

$$\boldsymbol{G_n}(x,x',s) = \sum_{m=0}^{\infty} \boldsymbol{a_m}(x',s)\phi_m(x),$$

where as before the eigenvalues and eigenfunctions are

$$
\begin{aligned}
\lambda_m &= \left(\frac{m\pi}{l}\right)^2, \\
\phi_m &= A_m \cos\frac{m\pi x}{l}.
\end{aligned}
$$

The Green's function for 3.3 is a solution of the equation

$$\begin{aligned}
&\frac{d^2}{dx^2}\boldsymbol{G_n}(x,x',s)\\
&-\left(\boldsymbol{L}(x)\boldsymbol{C}(x)\left[s^2+2\mathrm{i}n\omega s-n^2\omega^2\right]+\boldsymbol{C}(x)\boldsymbol{R}(x)\left[s+\mathrm{i}n\omega\right]\right)\boldsymbol{G_n}(x,x',s)\\
&-\left(\boldsymbol{R}(x)+s\boldsymbol{L}(x)+\boldsymbol{L}(x)\mathrm{i}n\omega\right)^{-1}\frac{d}{dx}(\boldsymbol{R}(x)+s\boldsymbol{L}(x)+\boldsymbol{L}(x)\mathrm{i}n\omega)\frac{d}{dx}\boldsymbol{G_n}(x,x',s)\\
&=\delta(x,x')\boldsymbol{I_N}.
\end{aligned} \tag{3.4}$$

We substitute the expansion for $\boldsymbol{G_n}(x,x',s)$ into (3.4), multiply by $\phi_k(x)$ and integrate from 0 to l. This results in

$$\sum_{m=0}^{\infty}\left[-\lambda_k\boldsymbol{I_N}+\boldsymbol{K_{k,m}}(s)+\boldsymbol{H_{k,m}}(s)\right]\boldsymbol{a_m}(x',s)=\phi_k(x')\boldsymbol{I_N}$$

where

$$\begin{aligned}
&\boldsymbol{K_{k,m}}(s)=\\
&\int_0^l-(\boldsymbol{L}(x)\boldsymbol{C}(x)\left[s^2+2\mathrm{i}n\omega s-n^2\omega^2\right]+\boldsymbol{C}(x)\boldsymbol{R}(x)\left[s+\mathrm{i}n\omega\right])\phi_k(x)\phi_m(x)dx,\\
&\boldsymbol{H_{k,m}}(s)=\\
&\int_0^l-\phi_k(x)(\boldsymbol{R}(x)+s\boldsymbol{L}(x)+\boldsymbol{L(x)}\mathrm{i}n\omega)^{-1}\frac{d}{dx}(\boldsymbol{R}(x)+s\boldsymbol{L}(x)+\boldsymbol{L}\mathrm{i}n\omega)\frac{d}{dx}\phi_m(x)dx.
\end{aligned}$$

The number of eigenfunctions is limited to N_{mod}. This number is set in practical simulations to achieve a specified accuracy requirement.

$$\sum_{m=0}^{N_{\mathrm{mod}}}\left[-\lambda_k\boldsymbol{I_N}+\boldsymbol{K_{k,m}}(s)+\boldsymbol{H_{k,m}}(s)\right]\boldsymbol{a_m}(x',s)=\phi_k(x')\boldsymbol{I_N} \tag{3.5}$$

Equation (3.5) is enforced for $k=0..N_{\mathrm{mod}}$, resulting in

$$\left[-\boldsymbol{\lambda}+\boldsymbol{K}(s)+\boldsymbol{H}(s)\right]\boldsymbol{a}(x',s)=\underline{\boldsymbol{L}}(s)\boldsymbol{a}(x',s)=\boldsymbol{\phi}(x') \tag{3.6}$$

where

$$\begin{aligned}
\boldsymbol{\lambda}&=\mathrm{diag}(\lambda_0\boldsymbol{I_N},...,\lambda_{N_{\mathrm{mod}}}\boldsymbol{I_N}),\\
\boldsymbol{a}(x',s)&=\left[\boldsymbol{a_0},\boldsymbol{a_1},...,\boldsymbol{a_{N_{\mathrm{mod}}}}\right]^T,\\
\boldsymbol{\phi}&=\left[\phi_0(x')\boldsymbol{I_N},\phi_1(x')\boldsymbol{I_N},...,\phi_{N_{\mathrm{mod}}}(x')\boldsymbol{I_N}\right]^T.
\end{aligned}$$

The solution can be formed by diagonalising $\underline{\boldsymbol{L}}(s)$

$$\underline{\boldsymbol{L}}\boldsymbol{(s)}=\boldsymbol{Q}(s)\boldsymbol{\alpha}(s)\boldsymbol{Q}(s)^{-1}.$$

The diagonal elements $\boldsymbol{\alpha}(s)$ can be approximated by a polynomial in s over the frequency range of interest. In the uniform case,

$$\alpha_{uniform_j} = \mu_{LC}\left(s^2 + 2\mathrm{i}n\omega s - n^2\omega^2\right) + \mu_{CR}(s + \mathrm{i}n\omega) + \frac{j^2\pi^2}{l^2},$$

where μ_{LC} and μ_{RC} are the eigenvalues of the $N \times N$ matrices $\boldsymbol{LC}$ and $\boldsymbol{RC}$. Bearing this in mind, and remembering that the non-homogeneity is considered as a perturbation of the homogeneous case, the selected form of approximating polynomial may be set as $\alpha_j(s) = \alpha_{uniform_j}(s) + c_j$ where c_j is a constant fitted at a low frequency. This enables the inverse of $\underline{\boldsymbol{L}}\boldsymbol{(s)}$, denoted $\underline{\boldsymbol{L}}^{\boldsymbol{i}}(s)$, to be expressed as

$$\underline{\boldsymbol{L}}^{\boldsymbol{i}}(s) = \sum_{j=0}^{N\times N_{\mathrm{mod}}+1} \frac{1}{\alpha_j}\boldsymbol{Q_j}\boldsymbol{(}\boldsymbol{Q_j}^{-1})^T,$$

.

Hence,

$$\boldsymbol{a}(x', s) = \sum_{j=0}^{N\times N_{\mathrm{mod}}+1} \frac{1}{\alpha_j}\boldsymbol{Q_j}\boldsymbol{Q_j}^{-T}\boldsymbol{\phi}(x')$$

The Green's function is

$$\boldsymbol{G}(x, x', s) = \sum_{m=0}^{N_{\mathrm{mod}}} \boldsymbol{a_m}(x', s)\phi_m(x) = \sum_{m=0}^{N_{\mathrm{mod}}}\sum_{j=0}^{N_{\mathrm{mod}}} \underline{\boldsymbol{L}}^{\boldsymbol{i}}_{\boldsymbol{m,j}}(s)\phi_j(x')\phi_m(x),$$

where $\underline{\boldsymbol{L}}^{\boldsymbol{i}}_{\boldsymbol{m,j}}(s)$ is the (m, j)th $N \times N$ block of $\underline{\boldsymbol{L}}^{\boldsymbol{i}}$. Then $\boldsymbol{V_n}(x, s)$ is obtained as

$$\boldsymbol{V_n}(x, s) =$$
$$\int_0^l \sum_{m=0}^{N_{\mathrm{mod}}}\sum_{j=0}^{N_{\mathrm{mod}}} \underline{\boldsymbol{L}}^{\boldsymbol{i}}_{\boldsymbol{m,j}}(s)\phi_j(x')\phi_m(x)\left[-(\boldsymbol{R}(x') + \boldsymbol{L}(x')\mathrm{i}n\omega + s\boldsymbol{L}(x'))\boldsymbol{I_{sxn}}(x', s)\right] dx'.$$

Since

$$\boldsymbol{I_{sxn}}(x, s) = \boldsymbol{I_{s0n}}(s)\delta(x) + \boldsymbol{I_{sln}}(s)\delta(x - l),$$

$$\boldsymbol{V_n}(x, s) = \sum_{m=0}^{N_{\mathrm{mod}}}\sum_{j=0}^{N_{\mathrm{mod}}} \underline{\boldsymbol{L}}^{\boldsymbol{i}}_{\boldsymbol{m,j}}(s)\phi_m(x) \times$$
$$\left[-A_j(\boldsymbol{R}(0) + \boldsymbol{L}(0)\mathrm{i}n\omega + s\boldsymbol{L}(0)) \qquad - A_j(-1)^j(\boldsymbol{R}(l) + \boldsymbol{L}(l)\mathrm{i}n\omega + s\boldsymbol{L}(l))\right]\begin{bmatrix}\boldsymbol{I_{s0n}}(s)\\ \boldsymbol{I_{sln}}(s)\end{bmatrix}.$$

Therefore, the matrix representation for each mode n is

$$\begin{bmatrix} \boldsymbol{V_n}(0,s) \\ \boldsymbol{V_n}(l,s) \end{bmatrix} = \begin{bmatrix} \boldsymbol{Z_{n11}}(s) & \boldsymbol{Z_{n12}}(s) \\ \boldsymbol{Z_{n21}}(s) & \boldsymbol{Z_{n22}}(s) \end{bmatrix} \begin{bmatrix} \boldsymbol{I_{s0n}}(s) \\ \boldsymbol{I_{sln}}(s) \end{bmatrix}, \tag{3.7}$$

where

$$\boldsymbol{Z_{n11}}(s) = -\sum_{m=0}^{N_{\text{mod}}} \sum_{j=0}^{N_{\text{mod}}} A_m^2 \underline{\boldsymbol{L}}^{\boldsymbol{i}}_{\boldsymbol{m,j}}(s) \left[(\boldsymbol{R}(0) + \boldsymbol{L}(0)\mathrm{i}n\omega + s\boldsymbol{L}(0)) \right],$$

$$\boldsymbol{Z_{n12}}(s) = -\sum_{m=0}^{N_{\text{mod}}} \sum_{j=0}^{N_{\text{mod}}} A_m^2 (-1)^j \underline{\boldsymbol{L}}^{\boldsymbol{i}}_{\boldsymbol{m,j}}(s) \left[(\boldsymbol{R}(l) + \boldsymbol{L}(l)\mathrm{i}n\omega + s\boldsymbol{L}(l)) \right],$$

$$\boldsymbol{Z_{n21}}(s) = -\sum_{m=0}^{N_{\text{mod}}} \sum_{j=0}^{N_{\text{mod}}} A_m^2 (-1)^m \underline{\boldsymbol{L}}^{\boldsymbol{i}}_{\boldsymbol{m,j}}(s) \left[(\boldsymbol{R}(0) + \boldsymbol{L}(0)\mathrm{i}n\omega + s\boldsymbol{L}(0)) \right],$$

$$\boldsymbol{Z_{n22}}(s) = -\sum_{m=0}^{N_{\text{mod}}} \sum_{j=0}^{N_{\text{mod}}} A_m^2 (-1)^{m+j} \underline{\boldsymbol{L}}^{\boldsymbol{i}}_{\boldsymbol{m,j}}(s) \left[(\boldsymbol{R}(l) + \boldsymbol{L}(l)\mathrm{i}n\omega + s\boldsymbol{L}(l)) \right].$$

Note that $A_m = A_j$. As for the uniform case, the rational functions can be converted directly to pole-residue form and then converted to the time domain.

3.1 Example 1

The example is a single line of length 0.3m. The per unit length inductance varies as $L(x) = L_0 \mathrm{e}^{-\alpha x}$ and the per unit length capacitance varies as $C(x) = C_0 \mathrm{e}^{\alpha x}$. $L_0 = 50nH/m$ and $C_0 = 100pF/m$. The resistance varies as $R(x) = R_0 \mathrm{e}^{-\alpha x}$ and $R_0 = 10\Omega/m$. $\alpha = 4$. The input is

$$I_s(t) = \sin(\omega_1 t)\sin(\omega t) \qquad t \geq 0$$

$\omega_1 = 200\pi$ and $\omega = 2\pi \times 10^6$. Fig. 3.1 depicts the voltage at the sending-end of the open-circuit transmission line. The dotted line is the result from the proposed method with $N_{\text{mod}} = 50$. The solid line is the result when the transmission line is modelled in very fine uniform segments (100 sections) and the time-domain response is obtained using the numerical inverse Laplace transform. The result for a longer simulation is shown in Fig. 3.2. The red dotted line is the result from the proposed method. As for the uniform line, a very large number of time steps is required to simulate such a result using the numerical inverse Laplace transform. This number is determined by the high-frequency carrier unlike the proposed method where the high-frequency carrier is separated out.

3.2 Example 2

The second example is a coupled exponential line. The parameters are similar to those in (Manfredi et al. 2016) and are

$$\boldsymbol{L_0} = \begin{bmatrix} 171.4 & 18.65 \\ 18.65 & 171.4 \end{bmatrix} nH/m, \quad \boldsymbol{C_0} = \begin{bmatrix} 65.7 & -7.15 \\ -7.15 & 65.7 \end{bmatrix} pF/m, \quad \boldsymbol{R_0} = \begin{bmatrix} 10 & 0 \\ 0 & 10 \end{bmatrix} \Omega/m.$$

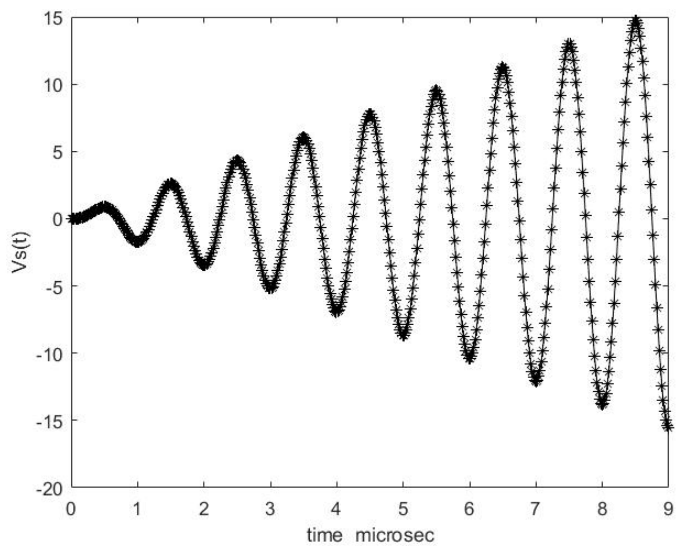

Figure 3.1: The voltage at the sending-end of the open-circuit transmission line.

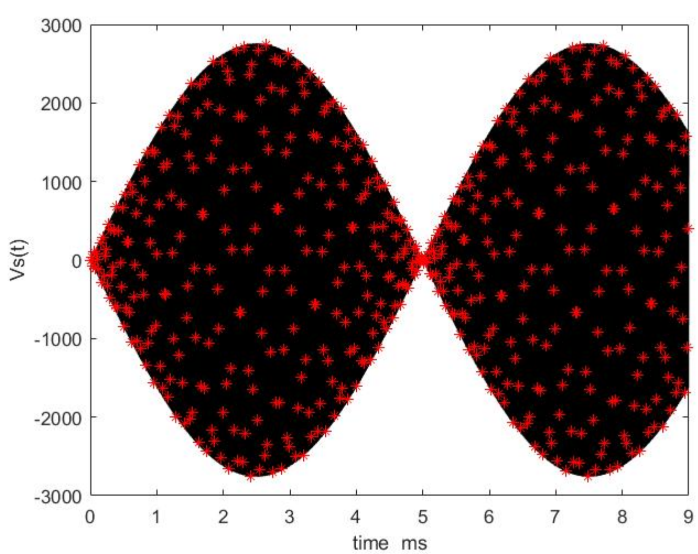

Figure 3.2: The voltage at the sending-end of the open-circuit transmission line on a longer time interval.

$$\boldsymbol{L}(x) = \boldsymbol{L_0}\mathrm{e}^{-\alpha x}, \quad \boldsymbol{C}(x) = \boldsymbol{C_0}\mathrm{e}^{\alpha x}, \quad \boldsymbol{R}(x) = \boldsymbol{R_0}\mathrm{e}^{-\alpha x}.$$

The line is 0.2m in length. The source current is again $\sin(\omega_1 t)\sin(\omega t)$ with $\omega_1 = 200\pi$, $\omega = 2\pi \times 10^6$ and $\alpha = 8$. Fig. 3.3 shows the voltage at the sending end of the energised line when all of the other terminals are open-circuit. The dotted line is the result from the proposed method with $N_{\mathrm{mod}} = 50$ and the solid line is the result when the transmission line is modelled in very fine uniform segments (100 sections) using the numerical inverse Laplace transform. The result for a longer simulation is shown in Fig. 3.4.

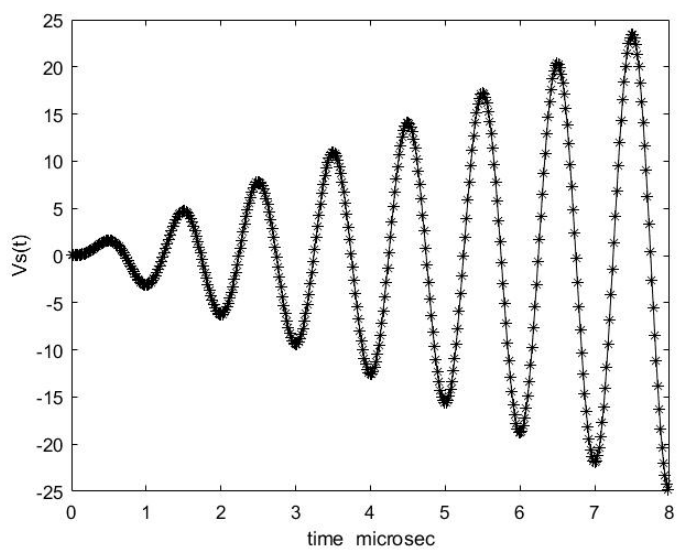

Figure 3.3: The voltage at the sending-end of the open-circuit coupled transmission line.

4 Conclusion

The paper has described a technique for forming a time-domain model for an interconnect when highly oscillatory modulated sources are present. The method separates the low-frequency information signal from the high-frequency carrier signal and this enables efficiencies to be gained. Results have highlighted the efficacy of the method for simulating modulated signals on both uniform and non-uniform interconnects. Results are validated by comparison with accurate results obtained using the numerical inverse Laplace Transform for linear cases and the Wendroff method for a nonlinear example. The method is important for circuit and system design and testing when signals with widely-varying frequency content are present.

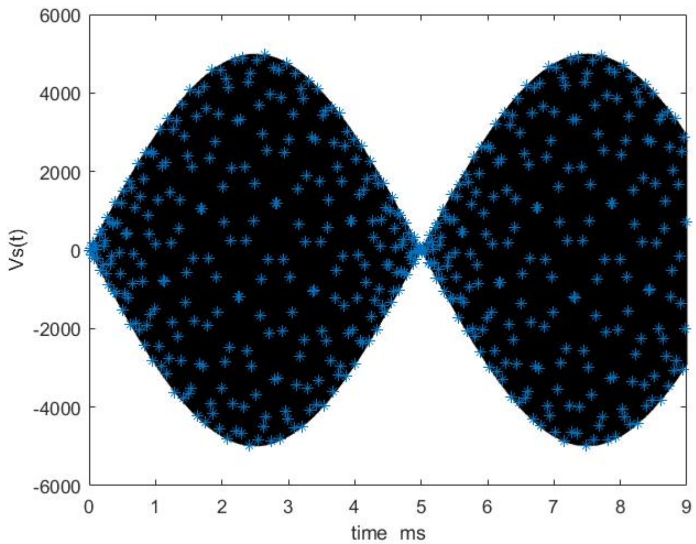

Figure 3.4: The voltage at the sending-end of the open-circuit coupled transmission line on a longer time interval.

References

Achar, R. (2011), 'High-speed interconnect modeling', *IEEE Microwave magazine,* pp. 61–74.

Afrooz, K. & Abdipour, A. (2012), 'Efficient method for time-domain analysis of lossy nonuniform multiconductor transmission line driven by a modulated signal using FDTD technique', *IEEE Transactions on Electromagnetic Compatibility,* **54(2)**, 482–494.

Altinbaçsak, S., Condon, M., Deaño, A. & Iserles, A. (2013), 'Highly oscillatory diffusion-type equations', *J. Comp. Maths,* **31(6)**, 549–572.

Antonini, G. (2012), 'Spectral models of lossy nonuniform multiconductor transmission lines', *IEEE Trans. on Electromagnetic Compatibility,* **54(2)**, 474–481.

Brančík, L. (2011), 'Time and Laplace-domain methods for MTL transient and sensitivity analysis', *COMPEL The international journal for computation and mathematics in electrical and electronic engineering* **30(4)**, 1205–1223.

Brančík, L. & Ŝevčík, B. (2011), 'Time-domain simulation of nonuniform multiconductor transmission lines in Matlab.', *International Journal of Mathematics and Computers in Simulation* **5(2)**, 77–84.

Chernobryvko, M., De Zutter, D. & Vande Ginste, D. (2014), 'Nonuniform multiconductor transmission line analysis by a two-step perturbation technique', *IEEE Transactions on Components, Packaging and Manufacturing Technology* **4(11)**, 1838–1846.

Dou, L. & Dou, J. (2011), 'Time-domain analysis of lossy multiconductor transmission lines based on the Lax-Wendroff technique', *Analog Integrated Circuits and Signal Processing,* **68(1)**, 85–92.

Jurić-Grgić, I., Lucić, R. & Bernadić, A. (2015), 'Transient analysis of coupled non-uniform transmission line using finite element method', *International Journal of circuit theory and applications,* **43**, 1167–1174.

Khalaj-Amirhosseini, M. (2006), 'Analysis of coupled nonuniform transmission lines using Taylor's series expansion', *IEEE Trans. Electromagn. Compat.,* **48(3)**, 594–600.

Lu, K. (1997), 'An efficient method for analysis of arbitrary nonuniform transmission lines', *IEEE Trans. Microwave Theory and Techniques,* **45(1)**, 9–14.

Manfredi, P., De Zutter, D. & Vande Ginste, D. (2016), 'Analysis of coupled exponential microstrip lines by means of a multi-step perturbation technique', *IEEE 20th Workshop on Signal and Power Integrity, Turin, Italy, 8-11, May 2016,* pp. 1–4.

Moreno, P., Gómez, P., Naredo, J. L. & Guardado, J. L. (2005), 'Frequency domain transient analysis of electrical networks including non-linear conditions', *Electrical Power and Energy Systems,* **27**, 139–146.

Nagaoka, N. & Ametani, A. (1988), 'A development of a generalized frequency-domain transient program-FTP', *IEEE Transactions on Power Delivery* **3(4)**, 1996–2004.

Tang, M. & Mao, J. (2007), 'Transient analysis of lossy nonuniform transmission lines using a time-step integration method', *Progress in Electromagnetics Research, PIER 69,* **69**, 257–266.

Tang, M. & Mao, J. (2008), 'A precise time-step integration method for transient analysis of lossy nonuniform transmission lines', *IEEE Transactions on Electromagnetic Compatibility* **50(1)**, 166–174.

Wilcox, D. (1978), 'Numerical Laplace transformation and inversion', *International Journal of Electrical Engineering Education,* **15(3)**, 247–265.

Yamamoto, S., Azakami, T. & Itakura, K. (1967), 'Coupled nonuniform transmission line and its applications', *IEEE Trans. Microwave Theory and Techniques,* **15(4)**, 220–231.